[illegible], Proc. 14th Conf. Radar. Meteor. , Abstract in BAMS, 51 (8), 1970.

ANALYSIS OF MESOSCALE PRECIPITATION AREAS

Pauline M. Austin and Robert A. Houze, Jr.

Massachusetts Institute of Technology
Cambridge, Massachusetts

1. INTRODUCTION

Subsynoptic-scale atmospheric motions and their relationship to synoptic-scale phenomena are recognized as having considerable meteorological significance (Charney et al., 1969). In general, these smaller-scale phenomena are difficult to evaluate by conventional meteorological methods of analysis because of the prohibitively dense observational networks required to describe them. Some of their effects, however, are readily observable in precipitation patterns as depicted by radar and rain-gauge data. The resolution of these instruments is particularly suitable for describing horizontal precipitation patterns ranging from those of the order of 10^4 km^2 in area which occur in cyclonic storms to ones as small as 1-10 km^2 associated with cumulus convection.

Rain areas of intermediate size, on the order of 10^2–10^3 km^2, are termed mesoscale and are observed quite frequently. In thunderstorms the intense cores of convective precipitation are surrounded by mesoscale areas of lighter rain. In widespread precipitation associated with synoptic-scale storms, also, numerous mesoscale areas of more intense precipitation containing cumulus-scale showers have been noted by Elliott and Hovind (1964, 1965), Matsumoto, Ninomiya and Akiyama (1967), Austin (1968), Browning and Harrold (1969) and Kreitzberg and Brown (1970). These patterns suggest that a whole range of small-scale phenomena occurs during rainstorms.

It seems, therefore, that an analysis of the precipitation and its variability in time and space might provide a fruitful approach to the study of at least some of the features of subsynoptic-scale air motions. The research presented here is an investigation of mesoscale precipitation areas and their relation to phenomena on the larger and smaller scales. It is hoped that this description will serve as a basis for realistic models of subsynoptic-scale air motions in rainstorms and for assessing the significance of these motions in the dynamics and energetics of the atmosphere.

2. DATA AND METHODS OF ANALYSIS

Basic data for these descriptions are PPI and RHI displays from the three radars formerly or presently in operation in the Department of Meteorology at M.I.T., and rain-gauge records from the field station in West Concord, Mass. Characteristics of the radars are summatized in Table 1. On all three the scope displays present quantized, averaged, range-normalized signal intensity with approximately 5 db in each intensity interval. A complete sequence of intensity levels is photographed every two to four minutes.

Table 1
Characteristics of weather radars at M.I.T.

	WR-66	SCR-615-B	AN/CPS-9
Wave length (cm)	10.5	10.7	3.2
Beam width (degrees between half-power points	1.3	3.0	1.0
Transmitted power (kw)	600	450	250

At the field station there are two tipping-bucket gauges which have time resolutions of a few seconds in heavy rain and about a minute in light rain. The more sensitive one tips for every 0.01 mm of rain. These gauges are regularly checked against each other and a weighing gauge. Agreement is generally within five per cent.

The data taken at M.I.T. are supplemented by the hourly precipitation amounts for New England, published monthly by the U.S. Weather Bureau for 69 gauges within 200 km of the radar site, and by the conventional meteorological observations.

In the first study eight storms were selected which had fair amounts of precipitation, good radar and rain-gauge coverage, and represented a variety of seasonal and synoptic situations. In these storms mesoscale precipitation areas and convective cells were identified from the intensity level sequences on the PPI. They were tracked for their entire lifetimes or as long as the data permitted. Dimensions, durations, intensities and motions of each were recorded; the intensities were checked with the rain gauge indications. Synoptic precipitation areas ($>10^4$ km^2) are not usually depicted to their full extent on the radars, and their existence and intensities were detected from maps of the hourly precipitation amounts.

In the second study a more objective analysis was attempted by computing the variance spectrum of the rainfall rates obtained from the field station gauges. A sampling interval of 30 sec was used. Techniques for computing and interpreting variance spectra are discussed in detail by Blackman and Tukey (1958) and, especially for geophysical applications, by Eddy et al. (1968).

3. ANALYSIS OF AREAL PRECIPITATION PATTERNS

The eight storms listed below were selected to

represent a variety of storm types. In no case was there specific knowledge of the precipitation pattern in a storm before it was chosen, nor was any storm rejected because of the patterns it was found to contain. The storm of 8 July 1963 was divided into two portions as indicated.

Date	Synoptic type
29 August 1962	Coastal low (ex-hurricane)
8 July 1963 (PF)	Occluded front moving eastward from Great Lakes, prefrontal precipitation
(F)	Same storm, frontal passage with squall line
18 May 1963	Coastal low moving from southwest with overland low to west
6 December 1962	Cyclone approaching from southwest
17 September 1963	Wave on stationary front
12 January 1963	Wave on stationary front
2 February 1963	Low moving from Great Lakes region
9 June 1965	Air mass thunderstorms

A precipitation area 10^4 km^2 or greater is assumed to be associated with a synoptic-scale system and is referred to as a synoptic area. A spot with an area on the order of 10 km^2 is assumed to represent a single cumulus convective element and is called a cell. A mesoscale precipitation area was therefore defined as one of intermediate size, i.e. larger than 50 km^2 and smaller than 10^4 km^2.

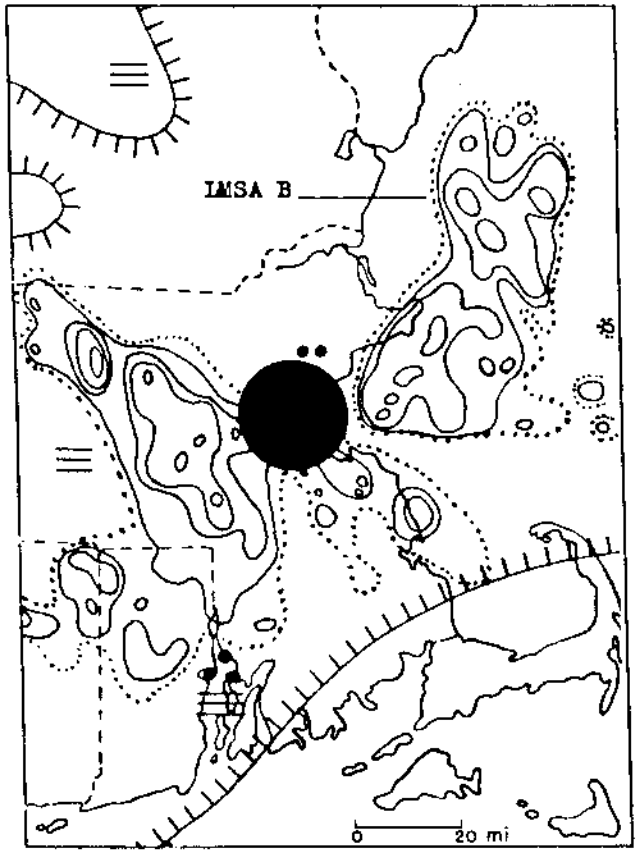

Fig. 1. Precipitation pattern for 0635 EST, 8 July 1963. Contours: 0(|||), 1(...), 2, 4, 8 and 16 mm hr^{-1}.

Early in the analysis, however, it became apparent that some of the precipitation patterns contained areas of two distinct sizes, both within the mesoscale range. These patterns showed several small mesoscale areas located within a larger but less intense one. The definition was therefore amended to distinguish between large mesoscale areas (LMSA's) which cover 10^3 to 10^4 km^2 and small mesoscale areas (SMSA's) which are 50 to 10^3 km^2 in area. Fig. 1 is an example of two large mesoscale areas each of which contains several small mesoscale areas and a number of cells.

Altogether, eight LMSA's, 25 SMSA's and 125 cells were subjected to systematic study. Results of the analysis are summarized below.

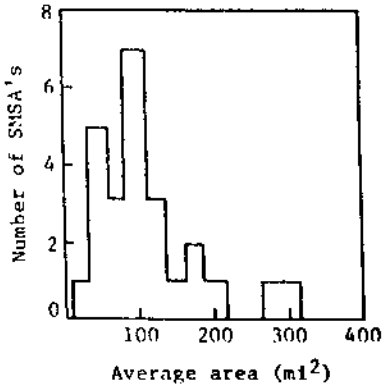

Fig. 2. Size distribution of small mesoscale areas.

a. Occurrence of Mesoscale Areas

Each of the seven cyclonic storms contained a synoptic area and many of the smaller-sized ones. The frontal band or squall line was of large mesoscale dimension and contained a number of SMSA's and cells. The thunderstorm complex was a small mesoscale area which contained a number of cells. Within a precipitation area of any given scale, areas of all the smaller scales were normally present. The average number of SMSA's within each LMSA at any given time varied from 3 to 6 with a density of 1 to 2 SMSA's per 1000 km^2. The number of cells varied from 1 to 7 per SMSA at one time with densities from 1 to 10 cells for each 100 km^2.

b. Horizontal Dimensions

An especially interesting result was that the observed size range for rain areas in each scale was considerably narrower than the one defined. Dimensions of cells are close to the limit of the radar resolution and could not be exactly determined, but most of them seemed to be 5-10 km^2 in area. For each mesoscale area, the size was observed at intervals during its lifetime and an average value obtained. Seventy-five percent of the SMSA's were between 100 and 300 km^2 (Fig. 2). All of the observed large mesoscale areas were between 1300 and 2600 km^2.

c. Durations

Typically the cells lasted only a few minutes, 0.1 to 0.5 hr; the SMSA's 0.5 to 3.0 hr with a median value of one hour; the LMSA's 2-5 hr; and synoptic areas longer than ten hours. One LMSA, the frontal band, was observed for 12 hours. Thus,

within an area of any given scale the pattern of smaller areas was constantly changing.

d. Intensities

Intensity of the precipitation in areas of any scale varied considerably from storm to storm, but their relative intensities were fairly consistent as shown in Table 2. Rainfall rate increased by approximately factors of two from synoptic area to LMSA to SMSA, while in the cells it was 2-10 times as great as in the surrounding small mesoscale areas. The actual amount of water deposited by typical large and small mesoscale areas and the percentages of it which came from various parts of the areas are shown in Table 3. Each type of area accounted for significant parts of the total rain, but the fraction within the cells was usually the smallest.

e. Vertical Extent

Precipitation in the mesoscale areas was assumed to extend as high as the weakest stratiform echoes which appeared in the RHI patterns on the same day. Since these echoes were detectable only to very short ranges, measurements could not be made in each specific mesoscale area. Vertical extent of the cells was also observed from the RHI displays; they were the same during any single storm but varied considerably on different occasions (Fig. 3). In the thunderstorm situations the cells extended throughout the depth of the surrounding precipitation and protruded above them, while in the cyclonic storms they were completely imbedded in the more widespread rain.

f. Motions

Observed velocities of the small mesoscale areas were the same as the average velocities of the

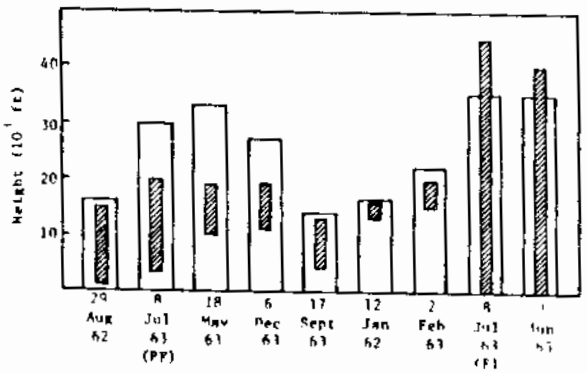

Fig. 3. Diagram showing for each storm the layer containing the cells (shaded) and the layer of lighter precipitation surrounding the cells (unshaded).

Table 2.
Rainfall rates in mm hr^{-1} for synoptic precipitation areas (R_S), large mesoscale areas (R_{LM}), small mesoscale areas (R_{SM}), and cells (R_C) in each storm.

Date	R_S	R_{LM}	R_{SM}	R_C
29 Aug 62	0.5-2	5	10	15-20
8 Jul 63 (PF)	0.5-1	2.5	5	10-40
18 May 63	0.2-0.5	2-3	5	10-15
6 Dec 62	0.5-1	*	3-6	10-50
17 Sep 63	0-Trace	0.5-1	2	4-15
12 Jan 63	0.5	*	1-2	3-4
2 Feb 63	0.5-1	*	2-3	5-10
8 Jul 63 (F)	none	0.5-5	5-25	20-100
9 Jun 65	none	none	5-20	45-90

*Could not be determined

Table 3.
Water deposited by various parts of the mesoscale areas.

P_{LM} = average volume of water per unit time from LMSA outside of SMSA's and cells.
P_{SM} = average volume of water per unit time from SMSA's outside of cells.
P_C = average volume of water per unit time from cells.

Units for total deposit: 10^7 m^3 hr^{-1}.

Date	Large mesoscale areas				Small mesoscale areas		
	Total Deposit	P_{LM} %	P_{SM} %	P_C %	Total Deposit	P_{SM} %	P_C %
29 Aug 62	32.7	22	69	9	8.0	91	9
					2.2	75	25
8 July 63 (PF)	10.4	51	44	5	1.8	87	13
	15.7	27	48	25	2.1	72	28
18 May 63	10.4	52	42	6	1.7	94	6
	7.1	33	65	2	1.0	95	5
6 Dec 62	not determined				2.1	46	54
					1.0	52	48
17 Sept 63	2.8	37	42	21	0.6	77	23
	3.4	29	55	16	1.0	92	8
12 Jan 63	not determined				0.6	79	21
					0.3	58	42
2 Feb 63	not determined				0.9	60	40
					0.7	84	16
8 July 63 (F)	31.2	11	54	35	3.9	60	40
9 Jun 65	no LMSA				3.7	37	63

cells which they contained, and were approximately the same as the velocity of the wind at mid-cell height (± 50% in speed, ± 25% in direction). Most of the large mesoscale areas also exhibited the same motions as the smaller areas within them. Two of the LMSA's moved differently. These two were bands whereas the others were all irregular or blob-shaped. The motions of the bands appeared to be related to those of the synoptic-scale systems with which they were associated.

g. Cell Characteristics

For cells there was a correlation between depth, duration and precipitation intensity, with 5000 ft in depth corresponding to about 8 mm hr^{-1} in intensity and 4 minutes in duration (Fig. 4).

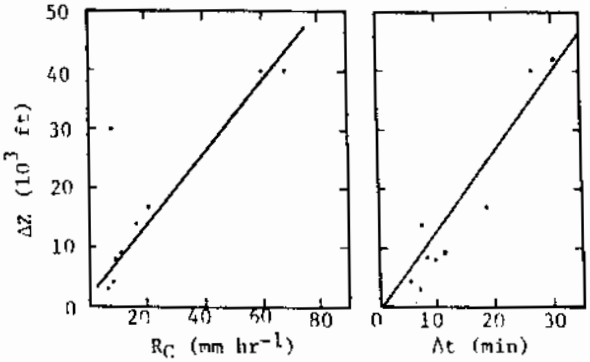

Fig. 4. Relation between cell depth (Δz), duration (Δt) and intensity (R_C). Each point represents an average cell in a particular storm.

Table 4.
Summary of characteristics of subsynoptic-scale precipitation areas.

Large mesoscale areas (LMSA)	Small mesoscale areas (SMSA)	Cells
	Occurrence	
Several within synoptic precipitation area	3-6 within LMSA	1-7 within SMSA
	Area	
1300-2600 km^2	250-400 km^2	5-10 km^2
	Duration	
2-5 hr	1 hr	5-30 min
	Rainfall rate	
two times rate in synoptic area	two times rate in LMSA	2-10 times rate in SMSA
	Vertical extent	
Cyclones: envelops cells		3,000-15,000 ft
Thunderstorms: not as high as cell tops		20,000-50,000 ft
	Motions	
Same as SMSA's within it (except for band shaped LMSA's)	Same as cells within it	Same as wind velocity at mid-cell height

The characteristics of precipitation areas of the various scales are summarized in Table 4. For each scale their dimensions, durations, and general behavior were remarkably similar even in storms with widely differing precipitation rates and synoptic characteristics.

Although there was some degree of subjectivity in the analysis and the number of storms somewhat limited, it is felt that the results are sufficiently consistent to leave little doubt that mesoscale precipitation areas of two distinct and rather narrowly-defined sizes as well as cumulus-scale cells occur in most storms.

4. VARIANCE SPECTRA OF RAINFALL RATE

Since within a given storm the subsynoptic-scale precipitation areas tend to move with the same velocity, one would expect that the record of rainfall rate at a point would reflect the spatial precipitation pattern. In particular, the variance spectrum would provide information regarding the regularity of the spacing between mesoscale areas or cells. For this analysis seven storms were selected which had rainfall records of ten hours or more. What is obtained for each storm is a plot of S, the normalized variance of rainfall rate per unit frequency, versus the frequency, n. An example is in Fig. 5. A flat or monotonically decreasing spectral curve indicates that the process sampled is random.

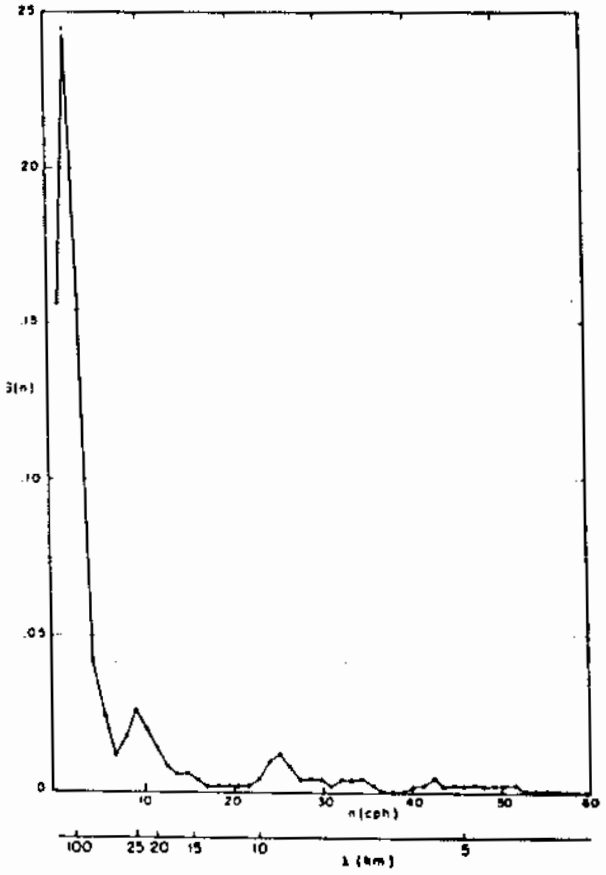

Fig. 5. Normalized variance per unit frequency, S(n), versus frequency, n, in cycles per hour for storm of 10-11 November, 1969. Lower scale is corresponding wavelength in km.

A flat spectrum indicates statistical independence of samples at successive time intervals, while a sharp upslope at low frequencies results from persistence or continued autocorrelation of the function over several intervals. Departures from a smooth curve, if they can be shown not to be merely sampling fluctuations, mean that the process which has been analyzed contains periodic functions as well as random ones.

Since the aim was to investigate the spatial characteristics, the frequency n was converted to a horizontal wavelength λ. The appropriate conversion for each storm was based on the motions of mesoscale precipitation areas as shown by radar and on the observed winds in the mid-low troposphere. These speeds differed considerably from storm to storm and ranged from 10 to 40 m sec^{-1}.

All of the computed spectra slope upwards sharply as λ increases (n decreases) indicating a high degree of persistence, or statistical dependence of successive 30-second observations, so that practically all of the total variance is contained by wavelengths of 5 km or greater. Each of the spectra has a number of maxima in this wavelength range as in the illustration in Fig. 5. The statistical significance of the peaks in any one storm was marginal at best, when judged by tests described by Blackman and Tukey (1958) and by Eddy (1968). What was examined, therefore, was the tendency for peaks to occur at the same wavelengths in different storms. Wavelengths at which peaks occurred were rounded off to the nearest 5 km and the number of peaks in each category was plotted in a histogram (Fig. 6). The histogram represents a weighted value rather than a simple count of the peaks in the seven spectra. The weighting was needed because some of the peaks were more prominent than others and also more spectral points are computed for a 5-km wavelength interval at small wavelengths than at large ones, as can be seen in Fig. 5, thus providing more opportunity for a peak to appear. Therefore, a peak in a particular 5-km interval was given a weighting directly proportional to the width of the peak and inversely proportional to the number of spectral estimates in that 5-km interval.

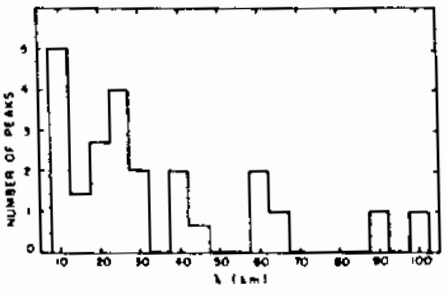

Fig. 6. Histogram showing where spectral peaks occurred in seven storms.

In Fig. 6, the two largest peaks are at λ = 10 km and λ = 25 km. These seem to be about the right distances to correspond to the spacings of the cells and small mesoscale areas described in the previous section, and suggest the possibility of a preferred spatial separation for precipitation areas of these scales. It should be noted, however, that the distances involved correspond to time intervals over the rain gauge which are comparable to the lifetimes of cells and mesoscale areas. Therefore the peaks in the spectra imply a tendency for a new precipitation area to develop upstream from a decaying one at the indicated distance rather than for two areas to coexist with that distance between them. Any conclusions must be extremely tentative, however, until more storms have been analyzed, and the implications in the combination of time and space patterns sampled by the rain gauge have been examined more closely.

5. CONCLUSION

This study has shown that rainstorms, even ones which differ greatly in intensity and general overall features, such as sharply defined squall lines and the rather amorphous widespread precipitation in many coastal cyclones, all comprise mesoscale areas and cumulus cells which have rather well-defined characteristics and behavior. The recognition of such basic components of precipitation areas is of considerable interest for several reasons.

In the first place, it provides a method for describing precipitation patterns in quantitative, meaningful and precise terms. For example, the synoptic-scale grid units are roughly 10^5 km^2 in area while significant features of the precipitation have dimensions as small as 1 km. Such features can be observed with a properly instrumented radar supplemented by several rain gauges with good time resolution. The precipitation pattern can be described adequately and objectively by giving the total amount of rain falling in the area, the number, intensity and vertical extent of large and small mesoscale precipitation areas and cells and their general configuration. The horizontal dimensions of these areas and the fact that elements of each scale are always located within areas of the next larger scale has already been established. Because of their transient nature, the exact location is not of importance except for very short-range local forecasts. Such a description is clearly much more compact and is also more informative than a listing of the intensity and height of precipitation echoes in each of 10^5 squares, 1 km^2 in area, and it has comparable resolution.

Second, the ubiquity of mesoscale precipitation areas opens up new challenges for research in precipitation processes because we do not know of physical lifting mechanisms on this scale, such as the larger-scale horizontal instability which produces broad areas of rising air in cyclones or the buoyancy which is responsible for smaller-scale "bubbles" in cumulus convection.

Most fundamental, perhaps, is the aspect pointed out earlier, the fact that the ability to observe at least some of the effects of subsynoptic-scale atmospheric motions in precipitation patterns provides a feasible approach to the problem of considering their significance in the entire spectrum of atmospheric motions and the transfers of energy and momentum from one scale to another.

Acknowledgement

The research reported in this paper was performed under National Science Foundation grant GA-10420.

References

Austin, P.M., 1968: Analysis of small-scale convection in New England. Proc. Thirteenth Radar Meteorology Conf., Boston, American Meteorological Society, 210-215.

Blackman, R.B., and J.W. Tukey, 1958: The Measurement of Power Spectra, Dover Publications, Inc., New York, 190 pp.

Browning, K.A. and T.W. Harrold, 1969: Air motion and precipitation growth in a wave depression, Quart. J. R. Met. Soc., 95, 288-309.

Charney, J.G., Chairman, and U.S. Committee for GARP, 1969: Plan for U.S. Participation in the Global Atmospheric Research Program, National Academy of Sciences, Washington, D.C., pp. 40-46.

Eddy, Amos, Claude E. Duchon and James A. Almazan, 1968: Variance Spectrum Analysis, Report No. 8, Atmospheric Science Group, College of Engineering, The University of Texas, Austin, 356 pp.

Elliott, R.D. and E.L. Hovind, 1964: On convection bands within Pacific coast storms and their relation to storm structure. J. Appl. Met., 3, (2), 143-154.

Elliott, R.D. and E.L. Hovind, 1965: Heat, water, and vorticity balance in frontal zones. J. Appl. Met., 4 (2), 196-211.

Kreitzberg, C.W. and H.A. Brown, 1970: Mesoscale weather systems within an occlusion, J. Appl. Met., 9, 417-432.

Matsumoto, S., K. Ninomiya and T. Akiyama, 1967: A synoptic and dynamic study on the three-dimensional structure of mesoscale disturbances observed in the vicinity of a cold vortex center. J. Met. Soc. Japan, 45 (1), 64-81.